

# Electro Magnetic Interference and HF Radio Receivers

June 4, 2023

## 1 Introduction

Throughout the 20th century HF radio receiver technology evolved with the aim of detecting distant, narrow band signals. Radio noise sets the limits of detection [10], and was assumed to be from natural sources or the receiver itself. However in the early 21st century, from lower HF right up to UHF noise from human activity now dominates the detection problem. We are no longer seeking to maximise signal-to-noise ratio (SNR), but signal to EMI ratio (SER).

We are slowly losing the ability to use analog SSB in urban areas. Many Hams report S9 noise levels,  $9 \times 6 = 54$  dB higher than a quiet S0 country station. Consequently, digital modes that can operate at low SERs are becoming popular. Digital modes are in an arms race with EMI.

Our target radio signals are from distant sources, weak, narrow band, and evolve slowly in time. Human generated radio noise tends to be very strong, wideband, with a time domain envelope that evolves quickly in time. It is often radiated from nearby sources, such as power lines and house wiring a few 10s of meters from our antenna. It has significant structure, so can be interpreted as an interfering signal, rather than random noise.

Modern radios are very good at removing unwanted narrowband signals, using frequency selectivity and good strong signal performance. This report explores the nature of human generated noise and explores techniques for reducing it's effects and increasing the SNR of received signals at urban locations.

## 2 Radio Noise Signals from Human Activity

Table 1 is a summary of human generated noise sources. The values are approximate and based on the authors experience - your mileage may vary! This categorisation gives us some insight that can be used to classify signals, consider their impact, and possible attacks.

The Time and Frequency columns describes the distribution of energy in time and frequency, for example power line arcing can cause clicks in our radio similar to atmospheric lightning. The noise signal consists of short, powerful

time domain pulses that are randomly distributed in time, resulting in wideband energy uniformly distributed in frequency. It may be identified and removed via noise blanking techniques.

In contrast DSL signals radiated from leaky phone lines looks like noise in the time domain and frequency domain, making it particularly hard to identify and remove. It is very similar to AWGN from natural noise sources.

Bandwidth relates the rate  $R$  of the noise pulses to the bandwidth  $B$  of a typical SSB HF receiver (around 2000 Hz). When  $R \ll B$ , we tend to hear individual noise pulses, and separate pulses can be observed in a time domain plot of the receiver output waveform. When  $R > B$ , we hear just a bandpass segment of the EMI signal, for example a tone from a PWM harmonic, or some modulated noise.

Our narrow band receiver smooths the time domain envelope of noise impulses. As  $R$  relative to  $B$  increase, our receiver smears the short time domain pulses (such as a PWM waveform) into a longer pulses with a smoother time domain envelope (such as damped sinusoids and in the limiting case AWGN noise), making the EMI signal harder to identify and remove.

For EMI signal to be detected by our receiver, we need a source of RF currents and a way of coupling those current into our antenna system (which includes the antenna and feed line). On lower HF our antenna systems are typically located less than one wavelength from the source of AC currents so both near and far field coupling is possible, and indeed a combination of both seems likely.

If we position our receiver some distance from many urban noise signals (for example the middle of an urban park), we get the sum of many signals added together, which converges to far field AWGN noise. The level reduces with distance, so an effective attack is decamping to a country location, and operating a portable station for the day.

Domestic electricity lines appear to operate in a mode part way between transmission line and antenna. RF does seem to propagate along them quite well, they then couple quite strong signals to nearby antennas. Likewise, DSL signals on ancient phone lines are poor transmission lines and and reasonably effective antennas, radiating significant local EMI. A home with buried electricity lines and fibre or wireless supplying Internet is an effective attack on these sources.

| Name       | Rate       | Time         | Frequency | Antenna      | BW      |
|------------|------------|--------------|-----------|--------------|---------|
| Power Line | 1 Hz       | random pulse | uniform   | power lines  | $R < B$ |
| Downlights | 50-60 Hz   | pulse train  | harmonics | house wiring | $R < B$ |
| SMPS       | 10-300 kHz | pulse train  | harmonics | house wiring | $R > B$ |
| DSL        | 1-12 MHz   | AWGN         | AWGN      | phone lines  | $R > B$ |
| Urban Sum  | lower HF   | AWGN         | AWGN      | power lines  | $R > B$ |

Table 1: Summary of Radio signals from Human Activity

The modulation used in our desired target signals is a factor. Digital modes

can operate at lower SNRs than analog SSB. Digital modes can also use Forward Error Correction (FEC), for example we can correct a bit error caused by a noise impulse wiping out one bit. Digital modulation also has a threshold effect - once the interference is a few dB lower than the wanted signals, it's impact on bit errors is small. FM, FSK & PSK are more robust to impulsive noise than amplitude modulated modes like SSB.

### 3 EMI from Pulse Trains

#### 3.1 Pulse Width Modulation

The PWM switch mode power supply is a ubiquitous source of interference. Consider the Fourier Series of an ideal pulse train [8]:

$$\begin{aligned} x(t) &= Ad + \frac{2A}{\pi} \sum_{n=1}^{\infty} \frac{\sin(\pi nd)}{n} \cos(n\omega t) \\ &= Ad + \frac{2A}{\pi} \sum_{n=1}^{\infty} \frac{x(t)}{n} \cos(n\omega t) \end{aligned} \tag{1}$$

where  $0 < d < 1$  is the duty cycle and  $\omega = 2\pi R$  the fundamental frequency. The Fourier series is a sequence of harmonics  $\cos(n\omega t)$ , with the amplitude of each harmonic set by the  $x(t)/n$  term. A typical value for  $R$  is a few kHz to several hundred kHz. For example with  $R = 70\text{kHz}$  and  $n = 101$  we will have a harmonic at 7.1 MHz. The  $1/n$  factor means the power of each harmonic falls off slowly with frequency, e.g. the  $n = 100$  harmonic will be just  $10\log_{10}(1/100) = -20$  dB down compared to the fundamental ( $n = 1$ ) power, and the  $n = 101$  harmonic almost the same power at  $10\log_{10}(1/101) = -20.043$  dB down.

If the duty cycle  $d$  is constant, then each harmonic is an unmodulated sine wave of constant amplitude. In practice  $d$  is time varying, as the duty cycle is continuously adjusted by the power supply. This leads to modulation of each harmonic  $x(t)$ , spreading the power to frequencies either side of the harmonic centre  $n\omega$ .

Let  $d$  have a constant and time varying component:

$$d = d_c + ad(t) \tag{2}$$

where  $d(t)$ ,  $|d(t)| \leq 1$  is a PWM modulation function and  $a$  is the peak amplitude of the modulation (ie the peak jitter of the PWM signal). For the  $n$ -th harmonic:

$$\begin{aligned} x_n(t) &= \sin(\pi nd) \\ &= \sin(\pi n(d_c + ad(t))) \\ &= \sin(\pi nd_c + \pi nad(t)) \\ &= \sin(\pi nd_c + h d(t)) \\ h &= \pi na \end{aligned} \tag{3}$$

It can be seen that  $h$  is strong function of  $a$ , as small changes are multiplied by  $n\pi$ . For example for  $n = 100, a = 0.01, h = \pi$ . Thus with just 1% jitter of the PWM signal, a cycle of  $d(t)$  would modulate over the entire  $\pm\pi$  range of the  $\sin()$  function.

We would like to estimate the spectrum of  $x(t)$ . First we consider small  $h \ll 1$ :

$$\begin{aligned} x_n(t) &= \sin(\pi n d_c) \cos(h d(t)) + \cos(\pi n d_c) \sin(h d(t)) \\ &\approx \sin(\pi n d_c) (1 - (h d(t))^2 / 2) + \cos(\pi n d_c) h d(t) \\ &\approx \sin(\pi n d_c) + h \cos(\pi n d_c) d(t) \end{aligned} \quad (4)$$

The LHS is a constant term related to the mean duty cycle of the PWM signal, the RHS is linear modulation term, i.e. a small linear modulation about a mean set point. When multiplied by the  $n$ -th harmonic  $\cos(n\omega t)$  in (1):

$$\begin{aligned} x_n(t) \cos(n\omega t) &= [\sin(\pi n d_c) + h \cos(\pi n d_c) d(t)] \cos(n\omega t) \\ &= \sin(\pi n d_c) \cos(n\omega t) + h \cos(\pi n d_c) d(t) \cos(n\omega t) \\ &= c_1 \cos(n\omega t) + c_2 d(t) \cos(n\omega t) \\ c_1 &= \sin(\pi n d_c) \\ c_2 &= h \cos(\pi n d_c) \end{aligned} \quad (5)$$

By examining the different frequency terms we can estimate the spectrum of the PWM signal near the  $n$ -th harmonic. Note  $c_1$  and  $c_2$  are constants that do not affect the number of different frequency terms. The LHS of (5) is a constant carrier term at the harmonic centre. The product of  $d(t) \cos(n\omega t)$  will produce images of the spectra of  $d(t)$  either side of  $n\omega$ . Thus (5) is Amplitude Modulated (AM) signal. For example if  $d(t)$  is a random variable with maximum frequency  $\omega_m$  radians, we would see a uniform noise spectrum over the interval  $n\omega \pm \omega_m$ , with a central "carrier" spectral line at  $n\omega$ . If  $\omega_m > \omega/2$ , the entire region between each harmonic will have additive white noise generated from the PWM signal.

For larger  $h$ , Equation 3 can be interpreted as Phase Modulation (PM) [7] of a zero frequency carrier. Assuming a random  $d(t)$ , the resulting spectra of  $x(t)$  can be approximated using Carsons Rule, as having 98% of it's power contained within  $B_c = 2(h+1)f_m$  Hz, where  $f_m$  is the maximum frequency component of  $d(t)$ . When multiplied by the  $\cos(n\omega t)$  term, the PM signal will spread the power of the carrier over range of adjacent frequencies, replacing the PWM carrier in the small  $h$  case with a wideband signal.

For example, let  $a = 0.02$  (a few percent jitter of the PWM duty cycle) and the bandwidth of the PWM control loop be  $f_m = 3$  kHz. At  $n = 100$  we have  $h = \pi n a = 2\pi$ , which implies a random deviation of  $\pm 2\pi$  (two cycles of  $\sin()$ ), and an  $x(t)$  bandwidth of  $B_c = 2(2\pi + 1)f_m = (4\pi + 2)f_m = 43$  kHz.

### 3.2 Discussion

1. Given  $h$  increases with  $n$ , we can expect to see AM type modulation either side of central harmonics lines at lower frequencies. At intermediate

frequencies a raised noise floor will be observed between harmonics. As the frequency increases further the power of the harmonics lines will reduce and gradually be replaced by broadband noise.

2. With the common scenario of a receiver of bandwidth  $B < R$ , we would encounter sine wave "carriers" every  $R$  kHz as we tune. Tuning between carriers would expect to hear a bandpass version of  $d(t)$ , this may or may not be white. If not white, it may have structure we can exploit.
3. With a large number of PWM sources, the central limit theorem suggests the sum will converge to AWGN noise with very little structure in time or frequency. This may be the case with signals radiated from electricity power lines that are coupled to thousands of switch mode power supplies in a city.
4. In the local case, it is possible that switch mode PWM or impulse noise may dominate a particular receiving station.

### 3.3 Periodic Impulse Noise

Section 3.1 explored the spectra of PWM power supplies which typically have a pulse rate  $R$  greater than the receiver bandwidth  $B$  (e.g.  $B = 2000\text{Hz}$  for SSB signals on HF radio). A low frequency pulse train (such as ignition or  $R = 50 \dots 60$  Hz impulses from domestic lighting) can also be interpreted as a pulse train with small duty cycle  $d$ , and  $R \ll B$ . In this case there will be a number of harmonics inside our receiver passband. Consider (1), band pass filtered such that only harmonics  $n_1 \dots n_2$  remain:

$$\begin{aligned}
 x(t) &= Ad + Ad \sum_{n=1}^{\infty} \text{sinc}(\pi nd) \cos(n\omega t) \\
 BPF[x(t)] &= Ad \sum_{n=n_1}^{n=n_2} \text{sinc}(\pi nd) \cos(n\omega t)
 \end{aligned} \tag{6}$$

Shifting down to baseband, and making the substitution  $k = n - n_1$ :

$$\begin{aligned}
 BPF[x(t)] \cos(n_1\omega t) &= \frac{Ad}{2} \sum_{k=0}^{n=n_2-n_1} \text{sinc}(\pi(k+n_1)d) \cos(k\omega t) \\
 &+ \frac{Ad}{2} \sum_{k=0}^{n=n_2-n_1} \text{sinc}(\pi(k+n_1)d) \cos((k+n_1)\omega t) \\
 &= b(t) + c(t)
 \end{aligned} \tag{7}$$

By applying a low pass filter we are left with the baseband term  $b(t)$ :

$$\begin{aligned} b(t) &= \frac{Ad}{2} \sum_{k=0}^{n=n_2-n_1} \text{sinc}(\pi(k+n_1)d) \cos(k\omega t) \\ &= \frac{Ad}{2} + \frac{Ad}{2} \sum_{k=1}^{n=n_2-n_1} \text{sinc}(\pi n_1 d + \pi k d) \cos(k\omega t) \end{aligned} \quad (8)$$

This expression is similar to the Fourier Series for a pulse train (1), but limited to  $n_2 - n_1$  harmonics by the bandwidth  $B$  of the receiver. The baseband signal  $b(t)$  can therefore be interpreted as a periodic signal with the same period  $\omega$  as the wideband periodic impulse noise  $x(t)$ . The shape of the pulse train will be a modified version of the  $x(t)$ , as we are using a band pass set of  $\text{sinc}()$  coefficients. Given the duty cycle  $d$  is likely to be small (e.g a  $10\mu\text{s}$  pulse every 20ms), and  $n_2 - n_1 \ll n_1$ , the coefficients are likely to be similar in amplitude across  $n_1 \dots n_2$ , producing a high peak to average power (low duty cycle) ratio pulse train.

Given  $d$  is small, and there is still significant power at high harmonic numbers,  $A$  must be very large for these impulse noise sources.

### 3.4 Attacks

1. Estimation and subtraction of the signals. Key take away is mirror of  $d(t)$  about harmonic centre. Estimation of signal from one sideband to cancel other, or from AM demodulation (envelope). This will be problematic when it's spread so far that we get energy from  $n+1$ ,  $n-1$  near harmonic  $n$ . However in that case it may not be as annoying/strong.
2. Estimation of signal from adjacent harmonics. Can we find  $x_n(t)$  from  $x_{n-1}(t)$ ?  $\omega$  and  $n$  can be estimated from the spectrum. A direct form solution is unlikely however the equations are differentiable so an iterative solution could be found.
3. Dual channel coherent removal (diversity receiver).
4. Noise blanking in the time domain. This may be challenging with  $R > 100$  kHz, as the period becomes  $< 10\mu\text{s}$ , implying the need for a wide bandwidth and sample rate  $>> 100$  kHz in order to resolve individual noise pulses in the time domain.
5. Training of time domain pulses, correlation and removal.

## 4 Noise Blanker

Consider a signal  $x(t)$  consisting of a wanted sinusoidal signal and an unwanted impulse train that repeats every  $1/R$  seconds.

$$x(t) = a_1 e^{j\omega_1 t} + a_{imp} \sum_{n=-\infty}^{\infty} \delta(t - n/R) \quad (9)$$

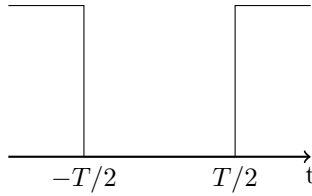
To remove the impulse, a blanking pulse train  $b(t)$  is applied. Each pulse is  $T$  seconds wide:

$$\begin{aligned} b(t) &= 1 - p(t) \\ p(t) &= \sum_{n=-\infty}^{\infty} \text{rect}(t - n/R) \\ \text{rect}(t) &= \begin{cases} 1, & |t| \leq T/2 \\ 0, & \text{otherwise} \end{cases} \end{aligned} \quad (10)$$

The blanking pulse train removes the impulse pulse train such that:

$$\sum_{n=-\infty}^{\infty} \delta(t - n/R) b(t) = 0 \quad (11)$$

Figure 1: Blanking Pulse  $b(t)$



The pulse train  $p(t)$  can be expressed as Fourier Series (1)

$$\begin{aligned} p(t) &= d + \frac{2}{\pi} \sum_{n=1}^{\infty} \frac{\sin(\pi n d)}{n} \cos(n\alpha t) \\ &= d + d \sum_{n=1}^{\infty} \text{sinc}(\pi n d) [e^{-j\alpha n t} + e^{j\alpha n t}] \\ &= d + dh(t) \\ h(t) &= \sum_{n=1}^{\infty} \text{sinc}(\pi n d) [e^{-j\alpha n t} + e^{j\alpha n t}] \end{aligned} \quad (12)$$

where  $\alpha = 2\pi R$  is the angular frequency of the pulse train,  $d = TR$  is the duty cycle, and  $h(t)$  is the RHS term containing the harmonics. The Fourier Transform of  $h(t)$  is:

$$\begin{aligned}
H(\omega) &= \int_{-\infty}^{\infty} h(t) e^{-j\omega t} dt \\
&= \int_{-\infty}^{\infty} \sum_{n=1}^{\infty} \text{sinc}(\pi n d) e^{-j\alpha n t} e^{-j\omega t} dt \\
&\quad + \int_{-\infty}^{\infty} \sum_{n=1}^{\infty} \text{sinc}(\pi n d) e^{j\alpha n t} e^{-j\omega t} dt \\
&= \sum_{n=1}^{\infty} \text{sinc}(\pi n d) [\delta(\omega + \alpha n) + \delta(\omega - \alpha n)]
\end{aligned} \tag{13}$$

The frequency shifted Fourier transform of  $h(t)e^{j\omega_1 t}$  is

$$\begin{aligned}
\int_{-\infty}^{\infty} h(t) e^{j\omega_1 t} e^{-j\omega t} dt &= H(\omega - \omega_1) \\
&= \sum_{n=1}^{\infty} \text{sinc}(\pi n d) [\delta(\omega + \alpha n - \omega_1) + \delta(\omega - \alpha n - \omega_1)]
\end{aligned} \tag{14}$$

Consider the output of the noise blanker:

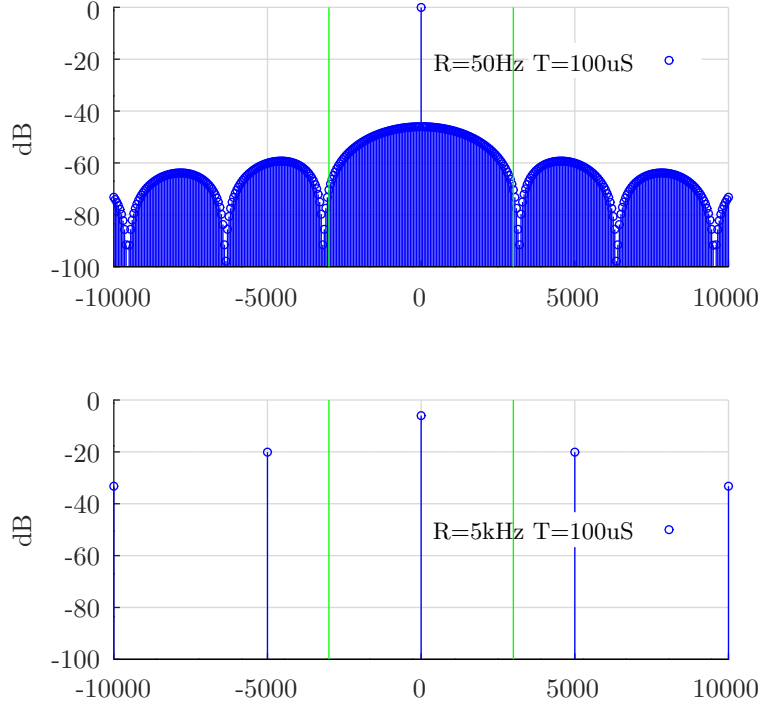
$$\begin{aligned}
y(t) &= x(t)b(t) \\
&= a_1 e^{j\omega_1 t} - a_1 e^{j\omega_1 t} p(t) \\
&= a_1 e^{j\omega_1 t} - a_1 e^{j\omega_1 t} (d + dh(t)) \\
&= a_1 (1 - d) e^{j\omega_1 t} - a_1 dh(t) e^{j\omega_1 t} \\
Y(\omega) &= a_1 (1 - d) \delta(\omega - \omega_1) - a_1 d H(\omega - \omega_1) \\
&= a_1 (1 - d) \delta(\omega - \omega_1) \\
&\quad - a_1 d \sum_{n=1}^{\infty} \text{sinc}(\pi n d) [\delta(\omega + \alpha n - \omega_1) + \delta(\omega - \alpha n - \omega_1)]
\end{aligned} \tag{15}$$

#### 4.1 Discussion

1. The wanted signal has been reduced to  $(1 - d)$ , and harmonics  $H(\omega)$  have been introduced either side. These are spectral copies of the input signal, spaced every  $\alpha$  radians/s.
2. An attenuation of  $(1 - d)$  is quite modest, for example if half of the signal is blanked ( $d = 0.5$ ), we lose just 3dB of the wanted signal. So quite heavy blanking is feasible, if it improves the output SNR by removing the noise pulse.



Figure 2: Two examples of Noise Blanker output spectrum  $|Y(f)|$ . The green lines show a sample SSB radio bandwidth of  $B = 3000$  Hz. Top is pulse rate  $R < B$ , bottom with  $R > B$ . Note the harmonic level increasing with duty cycle  $d = TR$ , and how the harmonics fall outside of  $B$  on the bottom plot.



3. The harmonic levels are proportional to the duty cycle  $d$ .
4. If the harmonic levels approach  $a_1$  they may cause interference. However for digital waveforms a margin of only a few dB beneath the wanted signal would be acceptable. This suggests digital waveforms can benefit more from noise blanking than analog.
5. A second, strong signal in the passband could introduce interference if one of its harmonic sidebands approaches  $a_1$  at  $\omega_1$ . This is the intermodulation effect of noise blankers.
6. The PWM analysis in Section 3 showed that a small duty cycle/small jitter signal can cause broadband noise. This suggests a narrow time domain

blanking pulse  $T \ll 1/R$  can remove that noise with acceptable impact on the wanted signal.

7. With noise/blanker pulse rates  $R > B$ , the harmonics are separated by  $R$ , so blanker harmonics are likely to be outside of our target pass band  $B$ . However intermodulation effects are larger, so strong signals further away could be aliased into our passband.
8. So far a rectangular blanking pulse has been assumed. A smoother function for  $p(t)$  is likely to reduce the level of  $H(\omega)$ .

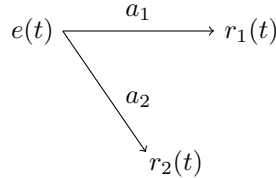
## 5 Antenna Systems

Noise signals can be induced in antenna systems and hence receivers by injection of common mode currents into feed lines. We should take steps to reduce coupling by routing feed lines away from EMI sources such as household wiring. The injection of common mode feed line currents into our receiver can be reduced by using balanced antenna systems and common mode chokes. A preamplifier located at the feedpoint may increase the ratio of wanted Rx signal to common mode feedline noise, depending on how the common mode signal is coupled into the antenna system.

Physical distancing of the antenna elements from noise sources will help reduce near field coupling more than far field, due to the strong relationship between near field strength and distance. However physical distancing is problematic on small urban blocks, where any antenna is likely to be less than one wavelength from conductors radiating EMI. Increased antenna height can help increase physical separation, if permitted by local government regulations.

### 5.1 Diversity

Figure 3: Diversity noise cancellation model



Consider an EMI signal  $e(t)$  received on two nearby antennas:

$$\begin{aligned} r_1(t) &= a_1 e(t) \\ r_2(t) &= a_2 e(t) \end{aligned} \tag{16}$$

where  $a_1$  and  $a_2$  are complex constants that model path loss and phase shift due to propagation delay. It can be shown that:

$$r_1(t) = cr_2(t) \quad (17)$$

where  $c = a_1/a_2$ , the ratio of two complex gains. Thus if we can estimate  $c$ , we can use (17) to estimate and remove the EMI  $r_1(t)$  received on antenna 1. To satisfy (17), we need to choose  $c$  to minimise the cost function:

$$E = r_1(t) - cr_2(t) \quad (18)$$

This model requires the EMI signal to be present (i.e. above the receiver internal noise) in both received signals. In diversity systems the two antennas are placed some fraction of a wavelength apart. Near field intensity is a strong function of distances of less than one wavelength, so the two antennas are likely to have very different responses to near field EMI. For example at a spacing of  $\lambda/4$  a near field signal coupled to one antenna may be undetectable in the other antenna. This implies the effectiveness of diversity will be very sensitive to antenna placement with near field EMI signals.

When suppressing far field EMI signals amplitude will be less sensitive to antenna placement. However this model also requires that the noise  $e(n)$  be a point source. Consider the case where there are several independent noise sources  $e_n(t)$  located at different locations, e.g. an urban location in the middle of a city. It is unlikely the phase and amplitude relationships will be the same for each source so the solution of (17) will be different for each source. If we rely on a single coefficient  $c$  cancellation will be ineffective. So the effectiveness of diversity will rely on how well the noise resolves to a single point source.

## 5.2 Directional Antennas

Consider a isotropic antenna that receives power equally from all directions. The gain pattern can be visualised as a sphere of constant radius, with a solid angle of  $4\pi$  steradians. Now consider an ideal directional antenna with a cone shaped pattern that receives all its power from a solid angle of  $\theta$  steradians, and no power from any other angle. Its power gain is  $G = \frac{4\pi}{\theta}$ .

If the EMI is the sum of many sources it is likely to have equal power flux density in all directions. Consider an isotropic antenna placed at the centre of this field. If the total noise power received from an isotropic antenna is  $N$  watts, the noise power in a solid angle of  $\theta$  radians is  $N \frac{\theta}{4\pi}$  Watts, and the noise power at the directional antenna terminals is:

$$\begin{aligned} P &= N \frac{\theta}{4\pi} G \\ &= N \frac{\theta}{4\pi} \frac{4\pi}{\theta} \\ &= N \end{aligned} \quad (19)$$

Thus the noise power received by a directional antenna is the same as an isotropic antenna and the same in any direction. In contrast our far field

wanted signal is a point source. If that signal develops a power of  $S$  watts into an isotropic antenna, it will develop a power of  $GS$  watts at the terminals of our directional antenna. The S/N improvement using a directional antenna in a uniform EMI field is therefore improved by the antenna gain  $G$ .

If the EMI is a point source, we may be able to place it in a pattern null using a directional antenna or diversity/beamforming techniques, further improving the effectiveness of the attack.

### 5.3 Topologies

Antenna topologies may help reduce near field coupling. For example the conductors of physically small, non resonant loops and dipoles can be placed further away from near field sources compared to a full length dipole that must extend across the entire width of an urban block [5].

There is some experimental evidence that the loop in/on ground topology [9][4] increases SNR in suburban locations compared to traditional antennas such as dipoles. The low gain (e.g. -30 dB) is usable for Rx operation as noise external to the receiver generally dominates system noise figure at HF. It is a balanced design, and the use of common mode chokes on either end of the feedline is recommended.

How this antenna reduces EMI (as implied by the improved SNR) is unclear. It is possible that compared to a reference dipole, near field noise is reduced as it is attenuated more than far field signals by the low (or subterranean) placement of the antenna. It has some directivity, and a balanced design which is useful in rejecting common mode feedline currents. It's low placement may also increase physical distance to overhead power lines and nearby houses.

There are many subjective reports that small loop antennas (either tuned or untuned) provide significant reductions in EMI, by virtue of lower sensitivity to near electric fields at certain distances from the loop.

However despite many claims and subjective reports it seems likely that antenna topology alone cannot distinguish far field EMI (such as AWGN noise that is the sum of many noise sources in a city) from wanted signals.

## 6 Experimental Measurements

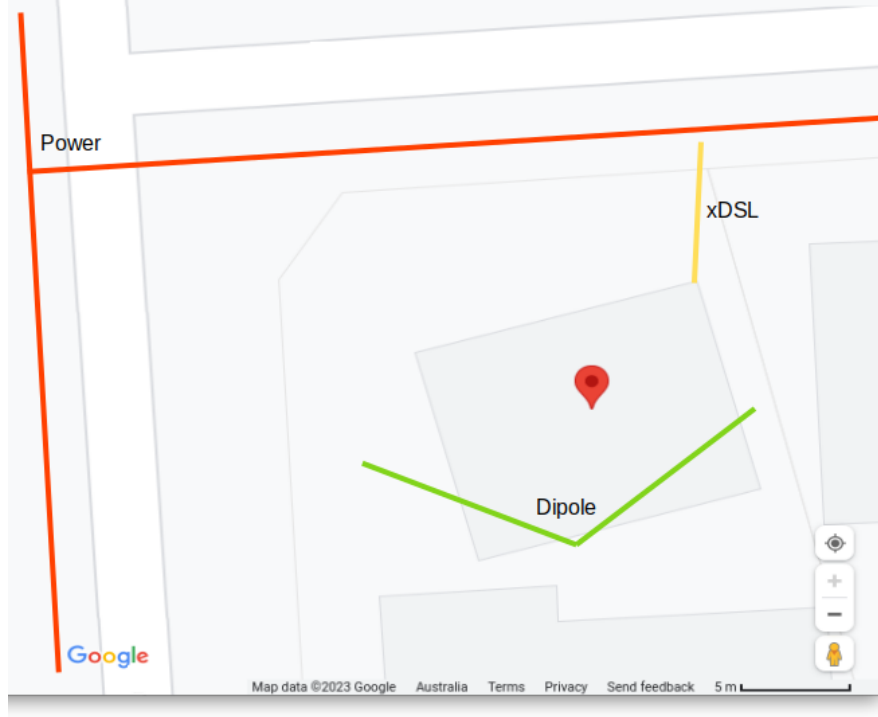
In May 2023 a some experimental work was conducted at the authors suburban home. The goal was to gain experience in measuring EMI and attempt to fit the experimental results to the theoretical framework above.

The home is located Adelaide (population 1.3 million), South Australia and is on a suburban square corner block of 550 m<sup>2</sup>. Overhead power lines are on two sides, and the suburb is served by VDSL Internet using overhead 70 year old phone lines. There are two adjacent houses, and the home has a 4 kW solar PV system.

The station antenna is an inverted V fan dipole with 40m and 20m elements, suspended over the house, the mast and feed point is 9m above ground. It is

coupled to 50 ohm coax using a balun at the feedpoint. Subjectively, SSB stations on the 40m band are hard to hear and unpleasant to listen to, and 20m varies between reasonable noise levels and completely unusable (time varying).

Figure 4: Map of the authors home station. EMI sources are power and xDSL lines, wiring in the home and adjacent homes, and a roof mounted solar PV system.

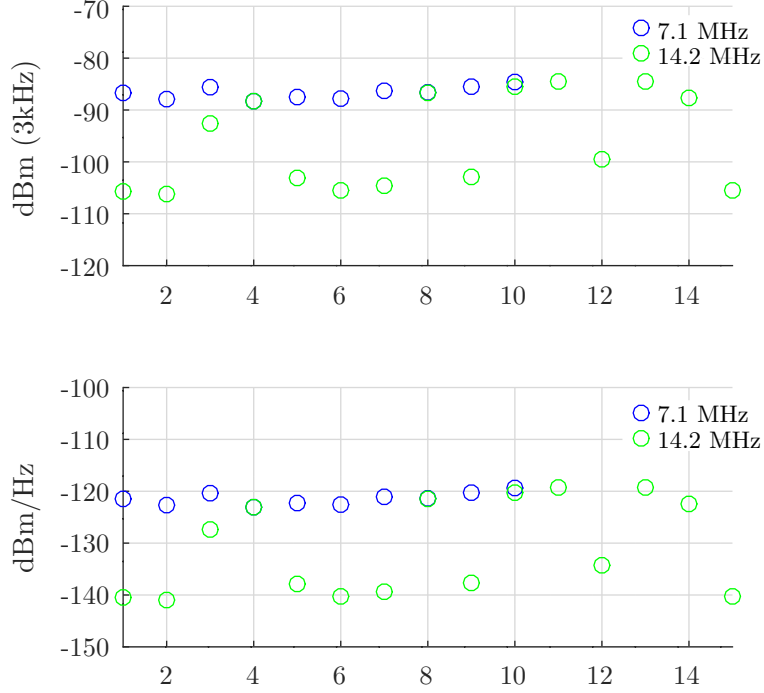


## 6.1 Observations

Figure 5 is a series of noise power measurements were made over a period of one week (1-3 measurements each day) in May 2023. The inverted V dipole was connected via a 3dB splitter to a Rigol DSA 815 spectrum analyser, and the noise power measured at 7.1 and 14.2 MHz. A 3kHz resolution bandwidth was used, span 200 kHz, the pre-amp was on, the attenuation set to 0, and the power averaged over 100 counts. The noise floor of the spec-an is about -160 dBm/Hz. The other port of the splitter was connected to an IC7300 HF radio to monitor the signal.

There were three clusters (Table 2). From the clusters the external noise figure is given by  $F_a = N_0 - 174$ , and calibrated S-unit  $S = N_0/6 + 27$ . Table

Figure 5: A sequence of HF noise power measurements over a period of 1 week, made in a 3 kHz resolution bandwidth (top), and converted to a 1 Hz bandwidth at bottom. The 7.1 MHz readings were high but quite stable, the 14.2 MHz noise fluctuated from acceptable to high, sometimes over a period of a few minutes



3 compares the measurements to the median  $F_a$  for residential locations from ITU-R P.372-12 [10, Fig. 10]. The measurements have been adjusted for the splitter (-3.5dB) and feedline (-1dB) losses. The noise field is assumed to be isotropic so the antenna gain is modelled as 0dB. The measured noise power is consistent with previous efforts by the author to measure urban noise using a small tuned loop [6].

## 6.2 Discussion

1. The IC7300 S-meter was found to be uncalibrated (6dB power change not equal to one S unit) and could not be relied upon to measure noise power. However the IC7300 waterfall is quite useful as a single plot shows both  $R < B$  impulse noise (lines across all frequencies) and  $R > B$  PWM

| Cluster | Freq (MHz) | $N_0$ (dBm/Hz) | $F_a$ Meas (dB) | S-unit |
|---------|------------|----------------|-----------------|--------|
| Nominal | 7.1        | -121           | 53              | S7     |
| Low     | 14.2       | -139           | 35              | S4     |
| High    | 14.2       | -125           | 52              | S7     |

Table 2: Measurement clusters and equivalent External Noise Figure  $F_a$  and S-units. The S-unit is derived from  $N_0$  assuming 6dB steps, S9=-73dBm, and a 3kHz noise bandwidth.

| Cluster | Freq (MHz) | $F_a$ P.372 (dB) | $F_a$ Meas (dB) |
|---------|------------|------------------|-----------------|
| Nominal | 7.1        | 49               | 53              |
| Low     | 14.2       | 41               | 35              |
| High    | 14.2       | 41               | 52              |

Table 3: P.372 Residential External Noise Figure  $F_a$  compared to Measurements

(harmonics spaced at  $R$  Hz).

2. The site has strong 50 Hz impulse noise however the IC7300 noise blanker removes this quite effectively. The zero span feature of the spec-an (set to 100ms sweep time) is useful for observing these short impulses - it turns the spec-an into a tuned oscilloscope with adjustable centre frequency and bandwidth. A sweep time of 100ms and resolution bandwidth of 30 kHz was useful for observing 10ms period pulses typical of 50 Hz impulses (one per edge).
3. In the "low/nominal" clusters AWGN noise floor was the dominant EMI signal, although at times PWM harmonics could be observed on both bands. The presence of the harmonics had no affect on the observed noise power between the harmonics, which suggests a small modulation index  $h$ .
4. The 14.2 high cluster corresponded to wideband noise with harmonics about 30kHz apart just visible on the waterfall. From our PWM analysis in Section 3, this suggests  $R > B$  with a fairly high modulation index  $h$ . The time varying amplitude (low and high clusters) could be due to shifts in the mean PWM duty cycle  $d$ , leading to shifts in the  $\sin(\pi nd)$  Fourier coefficients across the observed band. Given  $n$  is so high, even small shifts in  $d$  can cause large changes in the amplitudes of the Fourier components.
5. A 500MHz bandwidth oscilloscope with a 50 ohm input was connected instead of the spec-an but was not found to be very useful; nearby AM broadcast stations tend to dominate the wideband time domain signal.

### 6.3 Diversity Receiver

A set of experiments was conducted with the Linrad application [2] configured to use an Afedri AFE822x Dual channel SDR [1]. The second antenna was a

portable end-fed diople erected in the front of the property, about 10m from the inverted V dipole, sloping from 7m down to 2m.

Due to strong AM broadcast signals beneath 2 MHz, the AFE822x gain had to be reduced to avoid clipping, raising the noise floor of the receiver, and limiting the amount of diversity cancellation possible. The signals from both antennas were often quite different. This suggests signals local to each antenna such as near field EMI, or feed line pick up.

Using the Linrad phasing feature [3] it was possible to suppress signals that were common to both receivers, for example strong PWM harmonics. When tuned to segments of the "noise floor", suppression was not possible, which suggests the noise signals being received by both receivers were different.

An experiment was conducted where the signal from one antenna was split, and fed into each receiver. In this case, the noise could be suppressed by Linrad, demonstrating that if the noise in both receivers satisfies (17), it can be cancelled.

## 6.4 Further Work

The measurements suggest the dominant noise problem (2/3 clusters) is AWGN.  $R < B$  impulse noise is already being handled well by the IC7300, and the energy from occasional PWM signals in the low/nominal clusters seems localised to the harmonics (not affecting the AWGN noise floor between harmonics). If the EMI is AWGN, is it likely the sum of many urban EMI signals, which suggests far field. We cannot attack AWGN signals with blanking, as it has no time domain pulse structure.

This leaves diversity as a possible attack. This requires the EMI signals received by the two receivers to satisfy (17), implying the AWGN noise resolves to a point source.

So the next experimental steps are:

1. Set up a diversity system and attempt to suppress AWGN noise received in both antennas.
2. Use small, identical antennas placed close together to ensure similar received signals. Use physically small loops to enable placing them away from near field sources. Route feedlines away from the house, and consider common mode chokes.
3. Insert broadcast band filters into the diversity Rx inputs and measure noise figure to ensure our receiver noise floor is well below the target noise signals.
4. If AWGN noise can be suppressed, determine a method to measure SNR from far field test signals and determine if there is any improvement.



## References

- [1] Afedri AFE822x SDR-Net (Dual Channel). <https://www.afedri-sdr.com/index.php/new-afe822x-sdr-net-dual-channel>.
- [2] Linrad Home Page. <http://www.sm5bsz.com/linuxdsp/linrad.htm>.
- [3] Linrad, two channel reception, noise cancelling, antennas phasing. <https://www.sm5bsz.com/linuxdsp/run/phasing/linrad%20phasing%20window,%20v6%20open%20office.html>.
- [4] Loop in Ground for Rx only on low HF. <https://owenduffy.net/blog/?tag=lig>.
- [5] LZ1AQ Projects. <http://www.lz1aq.signacor.com/>.
- [6] Measuring HF Noise Around a City. <https://www.rowetel.com/?p=7964>.
- [7] Phase Modulation. [https://en.wikipedia.org/wiki/Phase\\_modulation](https://en.wikipedia.org/wiki/Phase_modulation).
- [8] Pulse Wave. [https://en.wikipedia.org/wiki/Pulse\\_wave](https://en.wikipedia.org/wiki/Pulse_wave).
- [9] The Loop on Ground Antenna. <http://www.kk5jy.net/LoG/>.
- [10] Recommendation P ITU. Itu-r p.372-12: Radio noise. Technical report, R-REC-P. 372/en.